

Dopant-induced stabilization of silicon clusters at finite temperature

Shahab Zorriasatein, Kavita Joshi, and D. G. Kanhere

Department of Physics, and Center for Modeling and Simulation, University of Pune, Ganeshkhind, Pune 411 007, India

(Received 8 September 2006; revised manuscript received 17 November 2006; published 19 January 2007)

With the recent advances in miniaturization, understanding and controlling the properties of technologically significant materials such as silicon in the nano regime assumes considerable importance. The silicon clusters in the size range of 15–20 atoms are known to be unstable upon heating. For example, Si_{20} does not melt but fragments around 1250 K, whereas Si_{15} has a liquidlike phase spread over a short temperature range and undergoes fragmentation at approximately 1800 K. In this paper, we demonstrate that it is possible to suppress such a fragmentation process by introducing the appropriate dopant (in this case Ti). Specifically, by using the first-principles density functional simulations we show that Ti-doped Si_{16} , having the Frank-Kasper polyhedral, remains stable till at least 2200 K and fragments only above 2600 K. Our calculations also indicate that the observed melting transition is a two-step process. The first step is initiated by the surface melting at approximately 600 K. In the second step, the destruction of the cage takes place at approximately 2250 K, giving rise to a peak in the heat capacity curve.

DOI: [10.1103/PhysRevB.75.045117](https://doi.org/10.1103/PhysRevB.75.045117)

PACS number(s): 31.15.Ew, 31.15.Qg, 36.40.Ei, 36.40.Qv

I. INTRODUCTION

With the advent of nanoscience and technology, investigating physical properties of clusters has assumed considerable importance. As the size of the system becomes smaller and smaller its physical and chemical properties are expected to change, sometimes significantly. In fact, this is what drives the quest for nano materials research. However, it may happen that this size effect drives a property towards an undesirable direction. The finite temperature properties of small silicon clusters is one such example. In our recent finite temperature studies¹ it was found that the small clusters of silicon (Si_n , $n=15$ and 20) become unstable and fragment when heated up to approximately 1500 K. Typically, our extensive density functional simulations showed that Si_{15} fragments at approximately 1800 K in to Si_9 and Si_6 , although we also observe $\text{Si}_{10}+\text{Si}_5$ and Si_8+Si_7 for a short time span. It exists in a liquidlike phase over a short temperature range (900 to 1400 K) before fragmenting. On the other hand, Si_{20} transforms from the ground state to the first isomer (with two distinct Si_{10} units) at approximately 1000 K and eventually fragments into two Si_{10} units at approximately 1200 K. Thus, Si_{20} does not show any solidlike to liquidlike transition prior to fragmentation. The result, although not surprising, can have technological implications, silicon being the key ingredient in most of the semiconductor devices. This paper addresses the issue of remedying this difficulty by using the appropriate dopant. That the impurities induce significant changes in the structure as well as the electronic properties is well known in the solid state community. In the context of clusters, several studies have been reported. For example, a single atom of tin or aluminum in lithium clusters is known to change the nature of the bonding among the host atoms.^{2,3} In a recent work, Mottet *et al.*⁴ demonstrated that a single impurity (Ni or Cu) in Ag_{55} cluster changes structural and thermal properties dramatically. Interestingly, this effect was found to be significant only in an icosahedral host.

Silicon is the most important semiconducting material in the microelectronics industry. In a small-size regime, the

structure and properties of materials often differ dramatically from those of the bulk. Over the past several years, there has been extensive theoretical and experimental work describing the ground state geometries of medium sized silicon clusters.^{5–10} These clusters are built upon stable tricapped trigonal prism (TTP) units which play a crucial role in the finite temperature behavior of the cluster.¹⁰ The high stability of TTP units results in fragmentation of these clusters instead of solidlike to liquidlike transition.¹ The ground state geometries of these clusters are well established in the literature. The ground state geometry of Si_{16} can be described as two fused pentagonal prisms.⁷

Recently, the electronic structure and the geometry of doped silicon clusters has attracted some attention. Experiments on doped silicon clusters Si_nM ($M=\text{Ti}, \text{Hf}, \text{Cr}, \text{Mo}$, and W) have shown large abundances for $n=15, 16$ and low intensities for other sizes.^{11–13} Specifically, the abundances drop drastically beyond $n=16$, giving support to the predictions of the exceptional stability of $n=16$ clusters. Kawamura *et al.*¹⁴ showed that for Si_nM , $M=\text{Ti}, \text{Zr}$, and Hf and $n=8–12$, basketlike open structures to be the most favorable, while for $n=13–16$, the metal atom is completely surrounded by silicon atoms. Recently, measurements of electron affinities of Ti-doped silicon clusters¹¹ have been found to have a minimum at $n=16$, suggesting the closed electronic shell nature and strong stability of Si_{16}Ti . The electronic structure of silicon clusters in the size range noted above has been studied by *ab initio* methods.^{5–7} It may be noted that none of the silicon clusters in this size range form stable caged structures. In a quest to obtain stable silicon cage structures, Kumar *et al.*^{14–17} found that it is possible to stabilize a caged structure for cluster using a class of dopants. Specifically, they showed that a single impurity of transition metal atoms such as Ti, Zr, Hf enhances the binding energy of Si_{16} and changes the structure to a caged one, similar to carbon cages. The gain in binding energy is substantial and is of the order of few eV, and highest occupied molecular orbital–lowest unoccupied molecular orbital (HOMO–LUMO) gap is more than 1 eV which make these structures stable. Among the systems studied, Si_{16}Ti has the largest

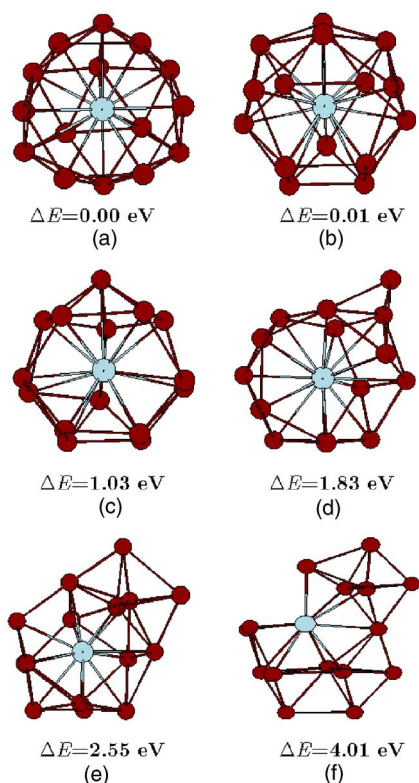


FIG. 1. (Color online) The ground state geometry and a few interesting isomers of Si_{16}Ti . ΔE represents the energy difference with respect to the ground state energy.

HOMO-LUMO gap (2.35 eV) as compared to other dopants of Si_{16} such as Zr and Hf.¹⁵ The ground state geometry for Si_{16}Ti has been found to be a Frank-Kasper polyhedron, which is also shown in Fig. 1(a). Therefore, Si_{16}Ti is a likely candidate to show a stable behavior at finite temperatures. The earlier studies reported the stability on the basis of the energies of the ground state structures and therefore are valid at zero temperature. It is of considerable practical interest to examine the stability of such clusters at finite temperatures and elucidate the possible mechanism for the dopant induced enhanced stability. As we shall demonstrate, by adding a dopant such as Ti, it is possible to avoid the fragmentation observed in small Si clusters. The cluster shows a surface melting of Si atoms. However, the motion of Si atoms is restricted to a small shell around Ti until 2200 K. The cluster is on the verge of fragmentation at approximately 2600 K, almost 1000 K higher than that in pure Si clusters.

II. COMPUTATIONAL DETAILS

We have carried out isokinetic Born-Oppenheimer molecular dynamic (BOMD) simulations using ultrasoft pseudopotentials within the generalized gradient approximation (GGA), as implemented in the VASP package.¹⁸ For computing heat capacities, the BOMD calculations were carried out for 17 different temperatures in the range of 100 to 3000 K, each with the duration of 150 ps or more, which result in a total simulation time of 2.6 ns. In order to obtain converged heat capacity curves especially in the region of

coexistence, more temperatures were required with longer simulation times. We have discarded the first 30 ps of each temperature for thermalization. To analyze the thermodynamic properties, we first calculate the ionic specific heat by using the multiple histogram (MH) technique.^{19,20} We extract the classical ionic density of states $[\Omega(E)]$ of the system, or equivalently the classical ionic entropy, $S(E) = k_B \ln \Omega(E)$ following the MH technique. With $S(E)$ in hand, one can evaluate thermodynamic averages in a variety of ensembles. In this work we focus on the ionic specific heat and the caloric curve. In the canonical ensemble, the specific heat is defined as usual by $C(T) = \partial U(T) / \partial T$, where $U(T) = \int E p(E, T) dE$ is the average total energy, and where the probability of observing an energy E at a temperature T is given by the Gibbs distribution $p(E, T) = \Omega(E) \exp(-E/k_B T) / Z(T)$, with $Z(T)$ the normalizing canonical partition function. We normalize the calculated canonical specific heat by the zero-temperature classical limit of the rotational plus vibrational specific heat, i.e., $C_0 = (3N - 9/2)k_B$.

We have calculated the root-mean-square bond length fluctuations (δ_{rms}) for Si-Si and Si-Ti bonds separately to compare the difference between them. The δ_{rms} is defined as

$$\delta_{\text{rms}} = \frac{1}{N} \sum_{i>j} \frac{(\langle r_{ij}^2 \rangle_t - \langle r_{ij} \rangle_t^2)^{1/2}}{\langle r_{ij} \rangle_t}, \quad (1)$$

where N is the number of bonds in the system ($N=120$ for Si-Si, and $N=16$ for Si-Ti), r_{ij} is the distance between atoms i and j , and $\langle \dots \rangle_t$ denotes a time average over the entire trajectory. Mean square displacements (MSD) are another traditional parameter used for determining phase transition and are defined as

$$\langle \mathbf{r}^2(t) \rangle = \frac{1}{NM} \sum_{m=1}^M \sum_{l=1}^N [\mathbf{R}_l(t_{0m} + t) - \mathbf{R}_l(t_{0m})]^2, \quad (2)$$

here N is the number of atoms in the system ($N=16$ for Si and $N=1$ for Ti), and \mathbf{R} is the position of the l th atom. Here we average over M different time origins t_{0m} , spanning over the entire trajectory. The interval between the consecutive t_{0m} for the average was taken to be about 1.5 ps. The MSD of a cluster indicate the displacement of atoms in the cluster as a function of time.

We have also calculated radial distribution function $[g(r)]$ and deformation parameter (ϵ_{def}). $g(r)$ is defined as the average number of atoms within the region r and $r+dr$. The shape deformation parameter (ϵ_{def}) is defined as

$$\epsilon_{\text{def}} = \frac{2Q_x}{Q_y + Q_z}, \quad (3)$$

where $Q_x \geq Q_y \geq Q_z$ are the eigenvalues, in descending order, of the quadrupole tensor

$$Q_{ij} = \sum_I R_{Ii} R_{Ij}. \quad (4)$$

Here i and j run from 1 to 3, I runs over the number of ions, and R_{Ii} is the i th coordinate of ion I relative to the center of mass (COM) of the cluster. A spherical system ($Q_x = Q_y = Q_z$) has $\epsilon_{\text{def}} = 1$ and larger values of ϵ_{def} indicates deviation

of the shape of the cluster from sphericity. We use the electron localization function (ELF) (Ref. 21) to investigate the nature of bonding. For a single determinant wave function built from Kohn-Sham orbitals ψ_i , the ELF is defined as

$$\chi_{\text{ELF}} = [1 + (D/D_h)^2]^{-1}, \quad (5)$$

where

$$D_h = (3/10)(3\pi^2)^{5/3}\rho^{5/3}, \quad (6)$$

$$D = (1/2)\sum_i |\nabla\psi_i|^2 - (1/8)|\nabla\rho|^2/\rho, \quad (7)$$

with $\rho \equiv \rho(\mathbf{r})$ is the valence-electron density. The ELF is defined in such a way that its value is unity for completely localized systems and 0.5 for homogeneous electron gas.

III. RESULTS AND DISCUSSION

We begin our discussion by noting the characteristics of the ground state (GS) and some low lying structures of Si_{16}Ti which are shown in Fig. 1. As has been already mentioned, the ground state of Si_{16}Ti is the Frank–Kasper polyhedron. The central Ti atom is surrounded by 16 Si atoms within two closely spaced shells, one with 4 Si atoms forming a tetrahedron and another shell consisting of 12 atoms. These shells are placed at 2.61 and 2.82 Å from the central Ti atom, respectively.

The first isomer [Fig. 1(b)] where all the Si atoms are nearly equidistant from the central Ti atom, is energetically very close to the ground state ($\Delta E=0.009$ eV). Isomers having either a distorted cage of Si atoms or without any Si cage are quite high in energy compared to the lowest two structures. The isomer shown in Fig. 1(f) occurs at very high temperature (around 2600 K) in our molecular dynamical runs, and indicates a possible path for fragmentation. At this point, it is interesting to compare the geometry and the electronic structure of pure silicon clusters with doped clusters. Si clusters have a very interesting growth pattern. The ground state geometries of Si_n till $n=22$ are prolate and for larger sizes the GS transforms into spherical structures. It has been also observed that a TTP unit is a part of prolate ground states. The presence of a highly stable TTP unit is responsible for bypassing the liquidlike state and leads to fragmentation of pure Si_n clusters around 1200 to 1800 K in the size range of 15–20. Further, the ground state of Si_{16} is a prolate structure and a cagelike isomer is found to be difficult to stabilize.

The nature of bonding in Si_{16}Ti and Si_{16} can be discussed by examining the isosurfaces of total charge density and ELF. We show the isosurface of ELF for the value of 0.55 and 0.70 in Figs. 2(a) and 2(b) for Si_{16}Ti , respectively. At higher values of χ_{ELF} , the figure clearly shows localization of the charge on the hexagonal rings depicting the covalent nature of the bonding. These atoms on the ring are connected to each other by the shortest bonds (2.37–2.43 Å) and are connected to the remaining four Si atoms at a low value of $\chi_{\text{ELF}} \approx 0.55$. The bonding between silicon atoms belonging to two different shells is metalliclike in the sense that it shows

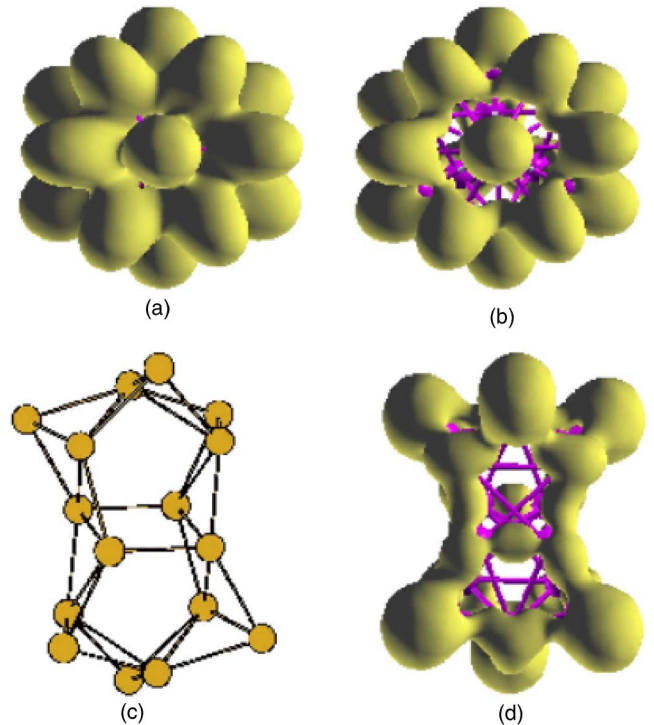


FIG. 2. (Color online) The isosurfaces of ELF for Si_{16}Ti at $\chi_{\text{ELF}}=0.55$ and $\chi_{\text{ELF}}=0.70$ are shown in (a) and (b), respectively. The ground state geometry and isosurfaces of ELF at $\chi_{\text{ELF}}=0.75$ for Si_{16} are shown in (c) and (d), respectively.

a delocalized charge distribution. This can be contrasted with the ELF for Si_{16} which is shown in Fig. 2(d) for the value of $\chi_{\text{ELF}}=0.75$, along with its GS geometry [shown in Fig. 2(c)]. For this value of χ_{ELF} , all atoms are connected via a single basin indicating that the Si-Si bond is stronger in Si_{16} compared to the one in Si_{16}Ti .

It is instructive to examine the differences in the first few shortest bonds in these two clusters. We show the first 30 shortest bonds (Si-Si) for these two systems in Fig. 3. Evidently the effect of the impurity after rearrangement is to increase the shortest bondlengths by 0.057 Å. This weakens the covalent bonding which is reflected in the ELF, as discussed above. There are 12 bonds with bond lengths of ≈ 2.6 Å in Si_{16}Ti that are formed between the atoms belong-

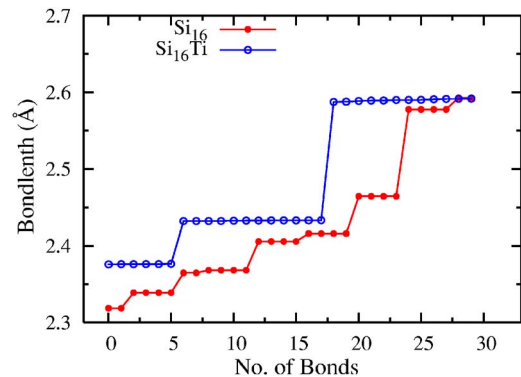


FIG. 3. (Color online) Comparing the first 30 bondlengths in Si_{16} and Si_{16}Ti . Si-Si bonds in Si_{16}Ti are weaker than those in Si_{16} .

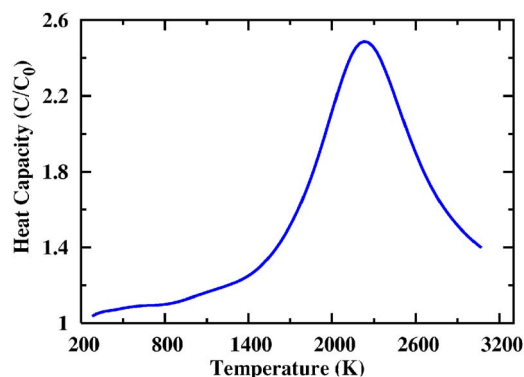


FIG. 4. (Color online) The heat capacity for Si_{16}Ti computed over the last 120 ps. The peak is at 2250 K.

ing to two different shells. As we shall see, the early diffusive motion begins because of these weaker bonds.

In short, Ti impurity changes the GS geometry of Si_{16} to a cagelike structure and the Si-Si bond is weaker in Si_{16}Ti . The impurity also enhances the HOMO-LUMO gap from 0.7 eV (for Si_{16}) to 2.35 eV (for Si_{16}Ti), and binding energy per atom from 4.62 eV (for Si_{16}) to 5.00 eV (for Si_{16}Ti). As we shall see, these differences lead to a significantly different finite temperature behavior of Si_{16}Ti .

In Fig. 4 we show the ionic heat capacity of Si_{16}Ti . The heat capacity displays a broad melting peak at 2250 K characteristic of a finite size system. A careful examination of the ionic motion and the traditional parameter such as δ_{rms} reveals that the main peak in the heat capacity is related to a complete breakdown of the Si cage and the escape of Ti atom from the cage. The δ_{rms} for Si-Si and Si-Ti bonds, shown in Fig. 5, brings out some interesting features. The value of δ_{rms} for Si-Si bonds is considerably high at lower temperatures (around 200 K), whereas the value of δ_{rms} for Si-Ti bonds is quite low till 1800 K. The higher value of δ_{rms} for Si atoms indicates that Si atoms are mobile at low temperatures. A detailed analysis of the ionic motion reveals that the cluster undergoes isomerization around temperatures as low as

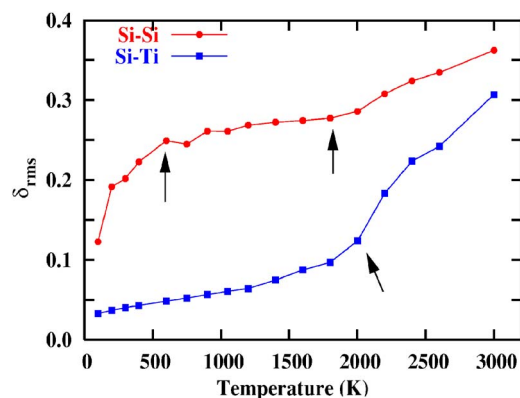


FIG. 5. (Color online) The δ_{rms} for Si-Si bonds (red) and Si-Ti bonds (blue) are shown. The region between 600 to 1800 K (shown by arrows for Si-Si bonds) corresponds to the “restricted” liquidlike behavior of Si cage. The rise in δ_{rms} observed after 2000 K (shown by arrows for the Si-Ti bonds) is associated with the breaking of the Si cage and diffusion of Ti through out the cluster.

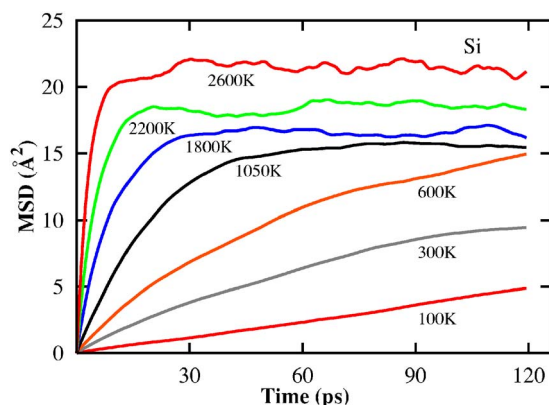


FIG. 6. (Color online) The MSD calculated for Si atoms for seven different temperatures.

100 K. The cluster transforms from the GS to the first isomer and back to the GS which in turn results in a diffusion of at least 4 atoms. The MSD also support this observation. In Figs. 6 and 7 the MSD computed for Si atoms and Ti atom at some relevant temperatures are shown. It can be noted from Fig. 6 that the MSD for Si atoms saturate around 600 K indicating that the atoms are diffusing on the spherical shell around Ti and the cluster is partially melted. On the contrary, as can be seen from Fig. 7, the Ti atom shows very small displacement till 2000 K. Although the MSD shows liquidlike behavior around much lower temperatures (600 K), the Si atoms are confined to a small shell around Ti (preserving the spherical shape) until quite high temperatures. Its only at approximately 2000 K that the Si cage breaks down, giving rise to a peak in the heat capacity at approximately 2200 K. That the motion of Si atoms is restricted to a shell is clear from the examination of the radial distribution function.

In Fig. 8 we show the radial distribution function calculated from the center of mass (Ti site) for some representative temperatures. The peak near origin is due to the Ti atom whereas a single peak around 2.8 Å is due to the Si cage. The width of this peak does not change significantly till 1600 K. A continuous distribution emerges after 2200 K indicating that the Si cage is destroyed and Ti has escaped from the cage. This change is accompanied by the change of the shape of the cluster.

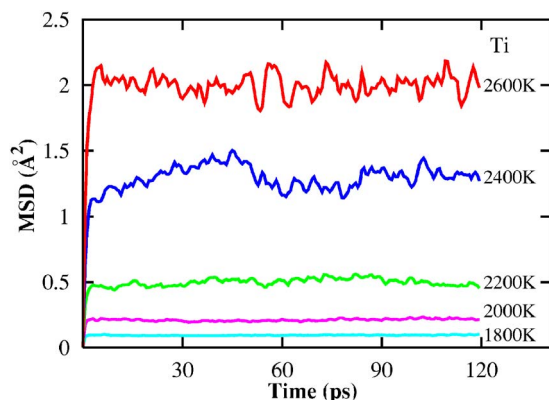


FIG. 7. (Color online) The MSD calculated for Ti atom for five different temperatures.

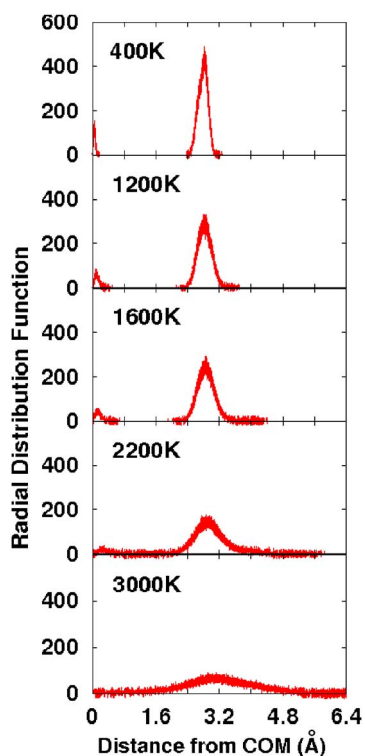


FIG. 8. (Color online) The radial distribution function calculated for Si_{16}Ti for five different temperatures. The peak near the origin is due to Ti atom.

In Fig. 9 we show the shape deformation parameter (ϵ_{def}) as a function of temperature. It can be seen that till 2000 K ϵ_{def} is nearly 1, indicating a spherical shape. The ϵ_{def} increases significantly above 2000 K indicating the breakdown of the Si cage. It turns out that a fragmentation channel opens up around 2600 K, possibly because of an emergence of a central Ti atom on the surface. We have observed that Si_{16}Ti at approximately this temperature fragments into two parts; the most probable fragments are $\text{Si}_{12}\text{Ti} + \text{Si}_4$ and $\text{Si}_{13}\text{Ti} + \text{Si}_3$. A typical configuration leading to fragmentation of Si_{16}Ti is also shown in Fig. 9.

IV. SUMMARY AND CONCLUSION

This work presents the ground state and finite temperature properties of Si_{16}Ti using density functional molecular dynamics simulation. The results clearly show the role of impurity in suppressing the fragmentation of Si_{16} .²² Contrary to

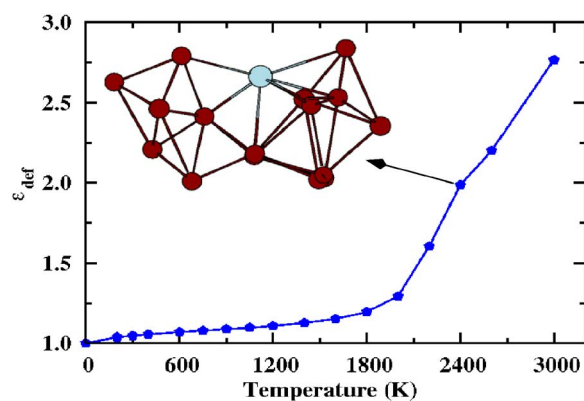


FIG. 9. (Color online) The deformation parameter is plotted as a function of temperature. Note the sudden rise in the deformation parameter after 2000 K. A typical configuration shown occurs at approximately 2400 K, and indicates a possible path for fragmentation.

the pure Si clusters, the doped cluster undergoes a solidlike to liquidlike transition, remaining stable at least up to 2600 K. However, the “melting” occurs in two steps: the first one is at quite low temperatures (approximately 600 K), where Si atoms diffuse on the shell, whereas the peak in the heat capacity (2250 K) is associated with the breaking of the Si cage and the escape of Ti atom from the cage. It is interesting to note that apart from changing the geometry significantly the impurity also changes the nature of the bonding. Interestingly, the Si-Si covalent bond is weaker in the impurity doped system. The binding energy per atom for Si_{16}Ti is higher by about 0.38 eV. This is a consequence of Ti-Si interaction.

Although there is insufficient data on the thermodynamics of clusters with impurities, we expect that whenever impurity induces a noticeable structural change, the finite temperature behavior of the cluster will change significantly. The present calculations demonstrate a possible way of tuning the finite temperature behavior of cluster using the appropriate dopant.

ACKNOWLEDGMENTS

K.J. and D.G.K. thank the Indo French Center for the Promotion of Advanced Research (IFCPAR) for partial financial support (Grant No. 3104-2). The authors also thank M.-S. Lee for many useful discussions. We thank X. C. Zeng for the coordinates of Si_{16} .

¹S. Krishnamurty, K. Joshi, D. G. Kanhere, and S. A. Blundell, Phys. Rev. B **73**, 045419 (2006).

²K. Joshi and D. G. Kanhere, J. Chem. Phys. **119**, 12301 (2003); M.-S. Lee, D. G. Kanhere, and K. Joshi, Phys. Rev. A **72**, 015201 (2005).

³H.-P. Cheng, R. N. Barnett, and U. Landman, Phys. Rev. B **48**, 1820 (1993).

⁴C. Mottet, G. Rossi, F. Baletto, and R. Ferrando, Phys. Rev. Lett. **95**, 035501 (2005).

⁵A. A. Shvartsburg, M. F. Jarrold, B. Liu, Z. Y. Lu, C. Z. Wang, and K.-M. Ho, Phys. Rev. Lett. **81**, 4616 (1998).

⁶I. Rata, A. A. Shvartsburg, M. Horoi, T. Frauenheim, K. W. Michael Siu, and K. A. Jackson, Phys. Rev. Lett. **85**, 546 (2000).

- ⁷X. L. Zhu, X. C. Zeng, Y. A. Lei, and B. Pan, *J. Chem. Phys.* **120**, 8985 (2004).
- ⁸K. A. Jackson, M. Horoi, I. Chaudhuri, T. Frauenheim, and A. A. Shvartsburg, *Phys. Rev. Lett.* **93**, 013401 (2003).
- ⁹L. Mitas, J. C. Grossman, I. Stich, and J. Tobik, *Phys. Rev. Lett.* **84**, 1479 (2000).
- ¹⁰J. Muller, B. Liu, A. A. Shvartsburg, S. Ogut, J. R. Chelikowsky, K. W. M. Sui, K-M. Ho, and G. Gantefor, *Phys. Rev. Lett.* **85**, 1666 (2000).
- ¹¹M. Ohara, K. Koyasu, A. Nakajima, and K. Kaya, *Chem. Phys. Lett.* **371**, 490 (2003).
- ¹²P. Sen and L. Mitas, *Phys. Rev. B* **68**, 155404 (2003).
- ¹³V. Kumar, T. M. Briere, and Y. Kawazoe, *Phys. Rev. B* **68**, 155412 (2003).
- ¹⁴H. Kawamura, V. Kumar, and Y. Kawazoe, *Phys. Rev. B* **71**, 075423 (2005).
- ¹⁵V. Kumar and Y. Kawazoe, *Phys. Rev. Lett.* **87**, 045503 (2001).
- ¹⁶V. Kumar and Y. Kawazoe, *Phys. Rev. B* **65**, 073404 (2002).
- ¹⁷V. Kumar, A. K. Singh, and Y. Kawazoe, *Nano Lett.* **4**, 677 (2004).
- ¹⁸Vienna AB INITIO simulation package (Technische Universität Wien, 1999); G. Kresse and J. Furthmüller, *Phys. Rev. B* **54**, 11169 (1996).
- ¹⁹A. M. Ferrenberg and R. H. Swendsen, *Phys. Rev. Lett.* **61**, 2635 (1988).
- ²⁰P. Labastie and R. L. Whetten, *Phys. Rev. Lett.* **65**, 1567 (1990).
- ²¹A. D. Becke and K. E. Edgecombe, *J. Chem. Phys.* **92**, 5397 (1990).
- ²²We have carried out a few representative MD runs in the relevant temperature range. We have estimated that Si₁₆ fragments around 1400 K.